

Waveguiding and confinement of light in semiconductor oxide microstructures

B. Méndez*, T. Cebriano, I. López, E. Nogales and J. Piqueras

Departamento de Física de Materiales, Facultad de Ciencias Físicas, Universidad Complutense de Madrid, 28040 Madrid, SPAIN

ABSTRACT

Interest on the control of light at the nano- and microscale has increased in the last years because of the incorporation of nanostructures into optical devices. In particular, semiconductor oxides microstructures emerge as important active materials for waveguiding and confinement of light from UV to NIR wavelengths. The fabrication of high quality and quantity of nano- and microstructures of semiconductor oxides with controllable morphology and tunable optical properties is an attractive challenge in this field.

In this work, waveguiding and optical confinement applications of different micro- and nanostructures of gallium oxide and antimony oxide have been investigated. Structures with morphologies such as nanowires, nanorods or branched nanowires as elongated structures, but also triangles, microplates or pyramids have been obtained by a thermal evaporation method. Light waveguide experiments were performed with both oxides, which have wide band gap and a rather high refractive index. The synthesized microstructures have been found to act as optical cavities and resonant modes were observed. In particular, photoluminescence results showed the presence of resonant peaks in the PL spectra of Ga₂O₃ microwires and Sb₂O₃ micro-triangles and rods, which suggest their applications as optical resonators in the visible range.

Keywords: waveguiding, optical cavities, resonant modes, semiconductor oxide microstructures

1. INTRODUCTION

A better understanding of light confinement in dielectric materials will enable to exploit devices based on optical microcavities¹. Recent research activities devoted to the fabrication and design of nano- and microstructures made of semiconductor oxides have paved the way to a wide range of applications. Besides the wide range of morphologies developed in semiconductor oxides, these materials allow several approaches to generate and confine light inside oxide microstructures. The challenge is to tune the doping and morphology/shape in order to make microstructures acting like optical cavities and eventually support resonant optical modes inside them. To achieve this goal, the sizes of the microstructures should match to light wavelengths in order to satisfy the interference boundary conditions, as for example is required in a Fabry-Perot interferometer. Optical resonant cavities of ZnO, GaN or In₂O₃ microstructures have been recently reported²⁻⁴. In some cases, laser emission has even been achieved in these media⁵. However, there are more oxide materials with promising potentialities in which issues concerning optical losses, emission wavelength range or quantum efficiency are still under investigation. Oxide materials with wide bandgap energies make possible optical confinement in a wide energy range. It is well known that optical active impurities and native defects play a major role in luminescence properties of oxide microstructures⁶. The next step is to establish the interplay of these intrinsic properties with morphology and shape features, which is a key factor in view of their applications as optical microcavities.

Thermal evaporation methods were used to grow several kinds of morphologies, from single nanowires and nanobelts⁷ to more complex structures such as hierarchical structures arising from self assembled processes⁸. In this work, we use both gallium oxide and antimony oxide to fabricate optical microcavities. In gallium oxide light is generated inside the microstructures due to the presence of optical active impurities⁹, and in antimony oxide the light arises from radiative transitions involving near band edge emission and levels related to native defects¹⁰. The studied structures are microwires of gallium oxide and microtriangles and microrods of antimony oxide, respectively. The experimental data support the occurrence of Fabry-Perot resonances in these structures.

*bianchi@ucm.es; phone +34 394 4746; fax +34 394 4547

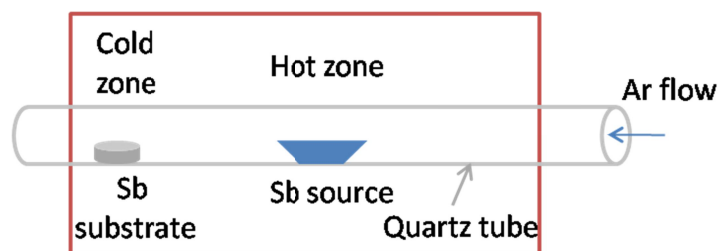


Figure 1. Sketch of the source and substrate arrangement inside the furnace to obtain Sb_2O_3 microstructures.

2. EXPERIMENTAL PROCEDURE

2.1. Synthesis of the oxide microstructures

The samples were obtained in an open furnace by oxidization of either metallic gallium or pure antimony sources under an argon flow. The substrates were gallium oxide and antimony compacted powders, respectively. It should be mentioned that no foreign catalysts were used to nucleate the microstructures and hence no undesired impurities were diffused into the structures. The key growth parameters are the temperature of substrate and source, the duration of the thermal treatment and the gas flow. Undoped Ga_2O_3 micro- and nanowires were first grown at 1100 °C for 15 hours, and Cr was then incorporated by thermal diffusion at 1500°C for 15 hours from chromium oxide powders to get Cr doped Ga_2O_3 microstructures^{9,11}. This second step does not modify the shape of the undoped microwires.

In the case of Sb_2O_3 , the source is placed at the hot temperature zone at 900 °C and the structures were formed at cold zones in the furnace. Figure 1 shows the sketch of the location of both substrates and sources inside the furnace. Microtriangles were formed on the antimony substrate at 420 °C, while microrods with rectangular cross-sections grew at the tube wall in a zone at a temperature of about of 550 °C. Further details of the growth procedure have been published elsewhere^{8,10}. Afterwards, both Ga_2O_3 microwires and Sb_2O_3 microrods were gently transferred to a silicon substrate for their physical characterization.

2.2. Characterization techniques

First characterization of the obtained samples was carried out in a FEI Inspec S50 or a Leica 440 scanning electron microscope (SEM) to analyze their morphology. Bruker X-ray microanalysis and electron back scattered diffraction (EBSD) systems were also available in these SEM equipments to investigate their compositional and micro-structural features. An AFM Nanotech instrument controlled by Dulcinea Software was used in the case of Sb_2O_3 microtriangles. In addition, X-ray diffraction (XRD) and transmission electron microscopy (TEM) analysis were also used to ascertain the crystalline quality of the structures.. Micro-photoluminescence (μ -PL) measurements have been performed in a Horiba Jobin Yvon HR800 Raman confocal microscope. The system used the 325 nm line of a HeCd laser as excitation source. In addition, a custom set up enables the deviation of the excitation laser spot from the collection point¹².

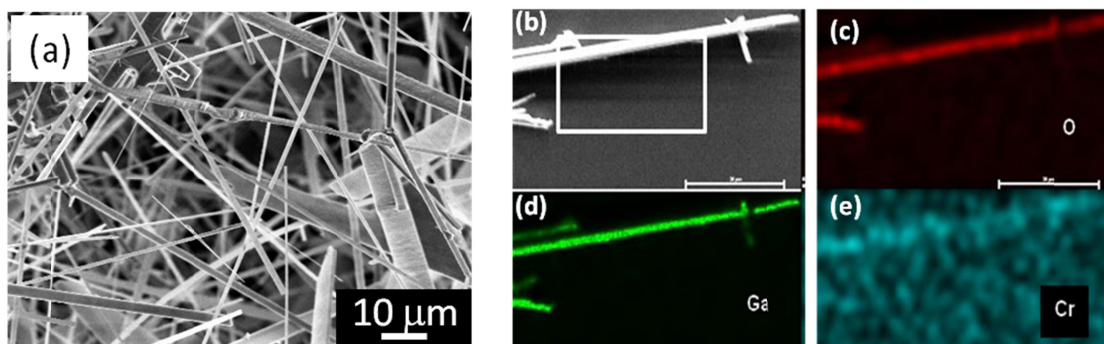


Figure 2. (a) SEM image of Cr doped Ga_2O_3 microwires. (b) - (e) SEM image and their corresponding element microanalysis mapping from O, Ga and Cr, respectively of a single doped Ga_2O_3 microwire.

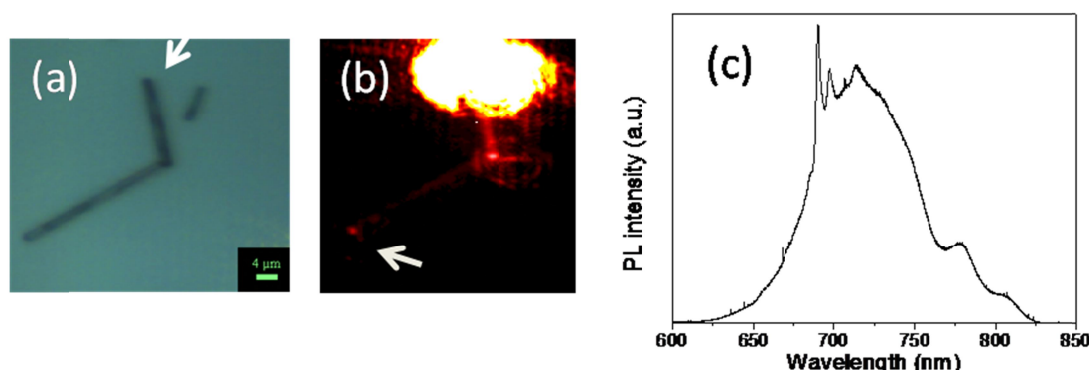


Figure 3. (a) Bright field optical image of a zigzagged Ga_2O_3 microwire, (b) micro-photoluminescence image and (c) PL spectrum of the emitted light.

3. RESULTS AND DISCUSSION

3.1. Gallium oxide microwires

A representative scanning electron image of Cr-doped Ga_2O_3 microstructures grown on the gallium oxide pellet is shown in Figure 2a. It can be observed that a high number of structures were formed as well as the occurrence of crossing and branched wires. The crystal quality of these structures was checked by X-ray diffraction, Raman spectroscopy and high resolution TEM analysis. The results showed that the microwires are of the monoclinic $\beta\text{-Ga}_2\text{O}_3$ phase and have a very high crystalline quality¹¹. Figure 2b shows the SEM image of an isolated Cr doped Ga_2O_3 wire and the corresponding chemical mapping of O, Ga and Cr. X-ray microanalysis spectra revealed the presence of Cr, but the concentration is very low, close to the detection limit of the system. However, as we will see this low Cr concentration is enough to produce a rather intense red luminescence at room temperature.

Some microstructures were transferred to a silicon substrate in order to study their luminescence and waveguiding properties under laser excitation. Gallium oxide has a wide band gap of 4.9 eV. However, deep energy levels originated by oxygen vacancies, either isolated or forming complexes with other point defects, provide radiative recombination paths across the energy gap. Undoped Ga_2O_3 usually exhibits an intrinsic ultraviolet-blue emission related to these native defect centers, as it has been previously assessed by photoluminescence¹³ and cathodoluminescence techniques¹⁴. In this work, we use as excitation source a laser line of 3.8 eV (325 nm), which does not excite luminescence related to native defects in Ga_2O_3 , but is suitable for exciting Cr^{3+} dopant ions. Figure 3 shows the bright field optical image and the corresponding micro-photoluminescence image of a bent Cr doped microwire. Under UV excitation at the upper end of the structure, indicated by the arrow in Figure 3a, red luminescence is generated by the Cr^{3+} ions in the gallium oxide matrix and guided following the microwire producing a bright red spot at the lower end (see the arrow in Figure 3b). The PL spectrum of the generated and propagated light is shown in Figure 3c and it corresponds to the sharp characteristic R lines at 696 nm and to the ${}^4\text{T}_2\text{-}{}^4\text{A}_2$ phonon assisted broad band observed at room temperature¹⁵. The refractive index, n ,

of Ga₂O₃ in this energy range is around 2.0¹⁶. This value is suitable to achieve total internal reflection in the wires in order to build up waveguides. In particular, it can be noticed from Figure 3b, that leakage of radiation after the corner is quite low, which indicates that these wires operate as efficient waveguides.

The next step is to consider these wires as potential optical microcavities or microresonators capable of storing light. To investigate this issue, red luminescence was generated by excitation with the laser at the middle point of a wire. This red light is confined in the microwire by their sharp ends acting as mirrors. As a consequence, Fabry-Perot (FP) resonances would occur for every light wavelength corresponding to an integer number of half-waves over the cavity length ($L = N \lambda/2n$, being n the refractive index). With the aid of the special setup in the confocal microscope, PL spectra at wire ends during excitation at the middle point of one microwire of 270 μm length were recorded, as Figure 4 shows. Bright red spots are clearly seen at both ends, which indicate that generated light is confined inside the wire. In addition, a careful examination of the PL spectra reveals a modulation over the whole spectra showing a set of maxima. The presence of these maxima suggests that Ga₂O₃ wires could be acting as optical resonators, if we consider their ends smooth enough to operate as reflecting optical mirrors. Figure 4c shows a detail of the PL spectrum between 722 and 730 nm, in which wavelength maxima are regularly separated by 0.47 nm. The expected separation between resonant maxima in an optical cavity of $L = 270 \mu\text{m}$ for modes of 724 nm of wavelength is 0.48 nm, which is in good concordance with that observed in the PL spectrum.

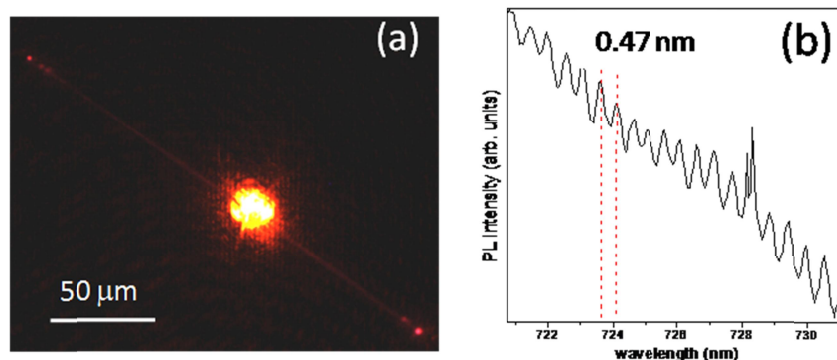


Figure 4. (a) micro-PL image and (b) PL spectrum of the emitted light recorded at the end of a Ga₂O₃ wire.

For Fabry-Perot cavity modes, the mode spacing $\Delta\lambda$ for a cavity with length L is given by $\Delta\lambda = \lambda^2/(2L n_g)$, where n_g is the group refractive index¹⁷. We have performed similar measurements in wires of different lengths and resonant maxima in PL spectra recorded at end points have been observed. At a fixed wavelength, the plot of $\Delta\lambda$ versus the inverse of the wire length fit well to a straight line⁹. From the slope of this line the group refractive index of Ga₂O₃ wires has been calculated giving a value of 1.99, which is consistent with those measured by other techniques. These results support the behavior of wires with lengths varying from 40 to 270 microns, suitable for light confinement of 690 to 780 nm wavelength.

3.2. Antimony oxide microtriangles

Sb₂O₃ exhibits two stable crystalline phases, the cubic phase or senarmonite¹⁸ and the orthorhombic phase or valentinite¹⁹, which appear depending on the temperature growth. An optical band gap of around 3.7 - 3.9 eV has been reported for the cubic phase²⁰, while a lower value (3.2 eV) has been estimated for the orthorhombic phase²¹. As far as their luminescence properties is concerned, antimony oxide would be of interest for applications in white light emission devices because of near band edge luminescence in the UV and a broad defect emission band from 400 to 650 nm (3.1 eV to 1.9 eV).

In accordance with the experimental procedure described above, Sb₂O₃ microtriangles grow on antimony substrates at 420 °C temperature. Figure 5a shows a representative SEM image of these structures. EBSD analysis of the triangles reveals the cubic phase with surfaces corresponding to the (111) planes. This morphology results from the self assembling of small triangles leading to either octahedral or more complicated polyhedral blocks. Dashed white triangles are depicted as an eye-guide in Figure 5a. Figure 5b shows the corresponding Atomic Force Microscopy (AFM) image of one these triangles and ordered tiny triangles with sizes of less than 200 nm can be resolved inside the bigger ones. It can also be noticed the self-similarity between both SEM and AFM images at different size-scales.

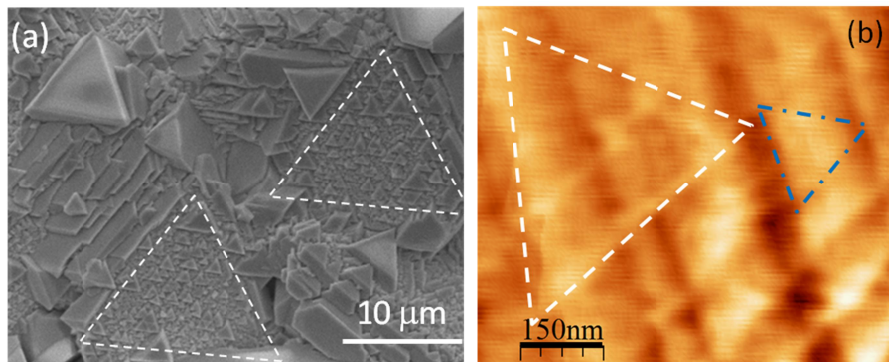


Figure 5. (a) SEM image of antimony oxide microtriangles. (b) AFM image of the same sample revealing the self similar triangle structure.

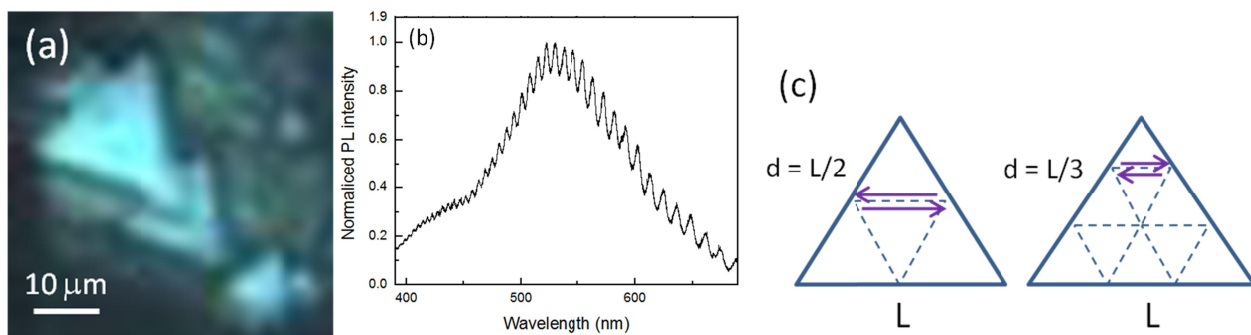


Figure 6. (a) Optical image of antimony oxide microtriangles, (b) PL spectrum recorded at the center of the triangle, and (c) possible optical paths inside the triangles.

In order to study the potential behavior of these micro-triangles as micro-resonators, we have studied the visible luminescence under the 325 nm (3.8 eV) laser excitation in the confocal microscope. Figures 6a and 6b show the optical image and the PL spectrum of the triangles, respectively. The emission comes from native defects of cubic Sb_2O_3 and consists of a broad band from 400 to 650 nm. Near band edge luminescence is not detected because of the filter used for the laser source. Overlapped to this band, pronounced wavelength maxima are resolved. This fact suggests that the micro-triangles are supporting optical resonant modes. Besides the FP resonances arising from reflections between parallel faces, whispering gallery modes (WGM) originated by total internal reflection are also possible in these structures. Chen *et al.*²² have reported mode characteristics of equilateral microcavities of GaInAsP, which show lasing behavior. The resonances appear on the basis of WGM in triangles. In our case, we observe resonant modes whose wavelength separation, $\Delta\lambda$, fits better to FP modes between triangle sides than to close trajectories inside the triangle as those shown in Figure 6c by dashed lines, which could be WGM modes¹⁰. The refractive index of antimony oxide from the literature is around 2.1 and exhibits dispersion in this wavelength range²³. $\Delta\lambda$ values are found to vary from 3 to 9 nm depending on the size of the triangle. The inner structure revealed by AFM images suggests that it is not easy to ascertain the light propagation path inside the triangles and internal reflections between the tiny triangles cannot be ruled out.

3.3. Antimony oxide microrods

In addition of the growth of cubic micro-triangles on the antimony substrate, a high amount of orthorhombic Sb_2O_3 microrods with rectangular cross-sections were also formed on the furnace tube walls at the 550°C temperature zone. The crystalline phase was determined by EBSD measurements in the SEM and orientation of the lateral surfaces of the microrods were resolved as (100) planes. Figure 7a shows a SEM image at low magnification of the obtained rods. A detail of one rod illustrating their cross-sectional dimensions is depicted in Figure 7b. Transversal sizes of the rods are in the range of units or tens of microns and their length is of several hundred microns. Figure 7c shows the PL spectrum recorded at the central point of the rod shown in Figure 7b. The observed band at 380 nm (3.26 eV) corresponds with the

near band edge luminescence of orthorhombic Sb_2O_3 . A modulation in the PL spectrum can be again resolved, with separation between maxima of 3.7 nm at $\lambda = 390$ nm. These resonances cannot be originated by interferences of light travelling along the longitudinal direction, as in the case of the previous Ga_2O_3 microwires, because they are very long. It seems more likely that reflections between the parallel faces at the cross-section would be the responsible for these resonant wavelengths. In particular, we have calculated the optical path from our experimental data and it gives 9.6 μm , which is close to the horizontal dimension of the rod. Similar data are obtained from other rods of different sizes. Therefore, our results suggest that resonances appear as a consequence of reflections between vertical faces of the rods.

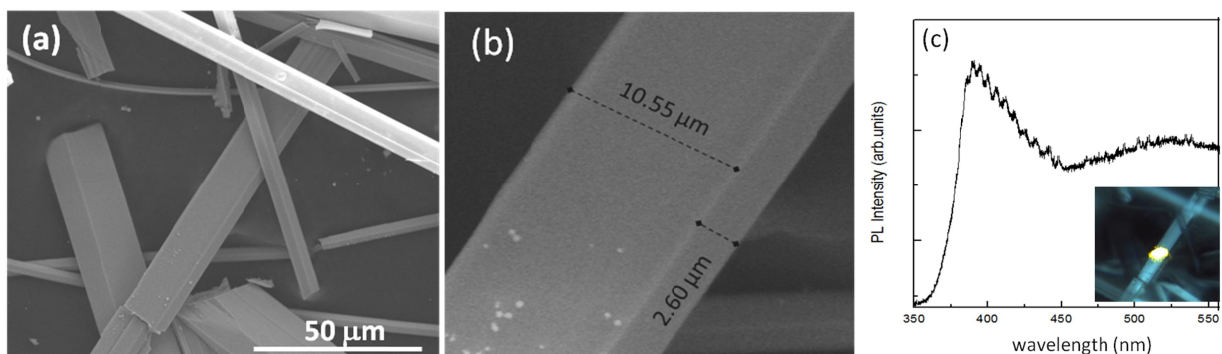


Figure 7. (a) SEM image of antimony oxide microrods. (b) Detail of one rod of 10.55 μm wide and 2.60 μm height. (c) PL spectrum recorded at the top part of the microrod. Inset: optical image of the rod.

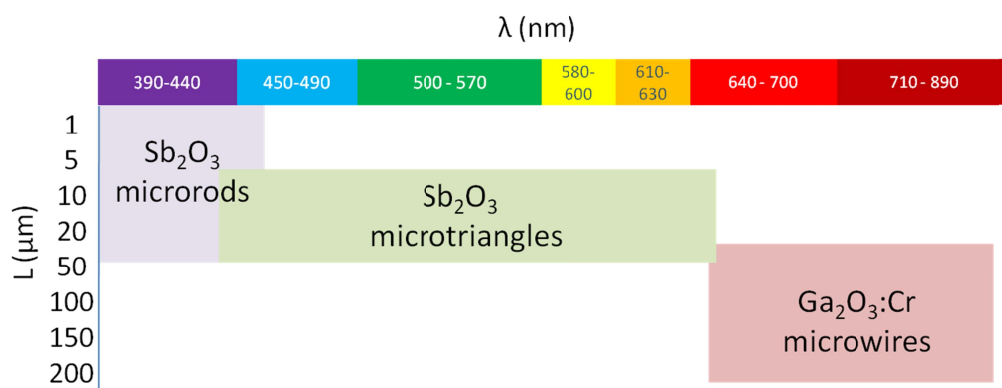


Figure 8. Sketch of the structures proposed as optical microcavities.

As a final issue for all the microstructures shown in this work, it should be noticed that the high crystalline quality and the presence of smooth surfaces are also key factors in order to prevent optical losses at reflection walls. Figure 8 summarizes the oxide microstructures studied by pointing out the wavelength of the light confined and the characteristic length, L , that provides the optical path leading to the resonances. In each case, a different dimension is considered as described in the previous sections. As a result, L can be considered the lateral dimension of the cross-section in rods, the triangle side for triangles, or the length of the microwires. This scenario enables us to support the potentiality of microstructures of the investigated oxides in applications for optical microcavities.

4. CONCLUSIONS

Gallium oxide and antimony oxides were investigated for light waveguiding in the whole visible range. Taking advantage of thermal evaporation methods, several morphologies of Ga_2O_3 and Sb_2O_3 semiconductor oxides were obtained and tested as optical microcavities. Micro-wires, triangles and rods have been successfully tested for light confinement and resonant wavelengths were observed at certain exit points. The light confined in these oxides microstructures comes from different luminescence mechanisms and covers almost the whole visible range. In the case of Cr doped Ga_2O_3 wires, red light is originated by the optically active Cr^{3+} ions, which are very efficient at room temperature in this host and provided optical resonances in the range from 690 to 780 nm. On the other hand, Sb_2O_3 is demonstrated to be of interest in the UV-blue range (380 - 450 nm) due to the near band edge luminescence of orthorhombic microwires, while defect related emission from cubic micro-triangles shows resonant peaks in the PL spectra at the intermediate region, 450 - 650 nm.

ACKNOWLEDGMENTS

This work has been financially supported by Spanish Government through MAT 2009 – 07882, MAT 2012- 31959 and CONSOLIDER CSD 2010 – 00013 projects.

REFERENCES

- [1] Vahala, K. J., "Optical microcavities" *Nature* 124, 839-846 (2003).
- [2] Wang, N.W., Yang, Y.H. and Yang, G.W. " Fabry–Pérot and whispering gallery modes enhanced luminescence from an individual hexagonal ZnO nanocolumn" *Appl. Phys. Lett.* 97, 041917-1 - 041917-3 (2010).
- [3] Schwartzberg, A.M., Aloni, S., Kuykendall, T., Schuck, P.J. and Urban, J.J. "Optical cavity characterization in nanowires via self-generated broad-band emission" *Optics Express*, 19, 8904-8911 (2011).
- [4] Dong, H., Chen, Z., Sun, L., Lu, J., Xie, W., Tan, H.H., Jagadish, C. and Shen, X. " Whispering gallery modes in indium oxide hexagonal microcavities" *Appl. Phys. Lett.* 94, 173115-1 - 173115-3 (2009).
- [5] Zimmler, M.A., Bao, J., Capasso, F., Müller, S. and Ronning, C. "Laser action in nanowires: Observation of the transition from amplified spontaneous emission to laser oscillation" *Appl. Phys. Lett.* 93, 051101-1 - 051101-3 (2008).
- [6] Nogales, E., López, I., Méndez, B., Piqueras, J., Lorenz, K., Alves, E. and García, J.A. "Doped gallium oxide for photonics" *Proc. of SPIE Vol 8263*, 82630B-1 – 82630B-7 (2012).
- [7] Wang, Z.L. "Nanobelts, Nanowires and Nanodiskettes of Semiconducting Oxides – from materials to nanodevices" *Adv. Mater.*, 15, 432-436 (2003).
- [8] Cebriano, T., Méndez, B. and Piqueras, J. "Micro- and nanostructures of Sb₂O₃ grown by evaporation-deposition: Self assembly phenomena, fractal and dendritic growth," *Mat. Chem. Phys.* 135, 1096-1103 (2012).
- [9] López, I., Nogales, E., Méndez, B. and Piqueras, J. "Resonant cavity modes in gallium oxide microwires," *Appl. Phys. Lett.* 100, 261910-1 – 261910-3 (2012).
- [10] Cebriano, T., Méndez, B. and Piqueras, J. "Study of luminescence and optical resonances in Sb₂O₃ micro- and nanotriangles," *J. Nanopart. Res.* 14, 1215-1 – 1251-8 (2012).
- [11] López, I., Nogales, E., Méndez, B., Piqueras, J., Peche A., Ramirez-Castellanos, J. and Gonzalez-Calbet, J. "Influence of Sn and Cr Doping on Morphology and Luminescence of Thermally Grown Ga₂O₃ Nanowires" *J. Phys. Chem. C*, (accepted).
- [12] Ma, R.M., Wei, X.L., Dai, L., Liu, S.F., Chen, T., Yue, S., Li, Z., Chen, Q. and Qin, G.G. "Light Coupling and Modulation in Coupled Nanowire Ring–Fabry–Pérot Cavity" *Nano Letters*, 9, 2697- 2703 (2009).
- [13] Binet, L. and Gourier D. "Origin of the blue luminescence of β-Ga₂O₃" *J. Phys. Chem. Solids*, 59, 1241-1249 (1998).
- [14] Nogales, E., Méndez, B. and Piqueras, J. " Cathodoluminescence from β-Ga₂O₃ nanowires" *Appl. Phys. Lett.* 86, 113112 (2005).
- [15] Nogales, E., García, J.A., Méndez, B. and Piqueras, J. "Red luminescence of Cr doped Ga₂O₃ nanowires" *J. Appl. Phys.* 101, 033517-1 - 033517-3 (2007).
- [16] Rebien, M., Henrion, W., Hong, M., Mannaerts, J.P. Fleischer, M. "Optical properties of gallium oxide thin films" *Appl. Phys. Lett.* 81, 250-1 250-3 (2002).
- [17] Duan, X., Huang, Y., Agarwal, R. and Lieber, C.M. "Single-nanowire electrically driven lasers" *Nature* 421, 241-245 (2003).
- [18] Svensson, C. "Refinement of the crystal structure of cubic antimony trioxide, Sb₂O₃" *Acta Cryst. B* 31, 2016-2018 (1975).
- [19] Svensson, C. "The crystal structure of orthorhombic antimony trioxide, Sb₂O₃" *Acta Cryst. B* 30, 458-461 (1974).
- [20] Tigau, N., Ciupina, V. and Prodan, G. "Structural, optical and electrical properties of Sb₂O₃ thin films with different thickness" *J. Optoelectron. Adv. Mater.* 8, 37- 42 (2006).
- [21] Deng, Z., Tang, F., Chen, D., Meng, X., Cao L., Zou, B. " A Simple Solution Route to Single-Crystalline Sb₂O₃ Nanowires with Rectangular Cross Sections" *J. Phys. Chem. B*, 110, 18225-18230 (2006).
- [22] Chen, Q., Hu, Y., Huang, Y., Du, Y. and Fan, Z. "Equilateral triangle- resonator injection lasers with directional emission" *IEEE J. Quantum Electron*, 43, 440–444 (2007).
- [23] Tigau, N., Ciupina, V. and Prodan, G. "The effect of substrate temperature on the optical properties of polycrystalline Sb₂O₃ thin films" *J. Cryst. Growth*, 277, 529–535 (2005).